

Simulation of borehole acoustic measurements in axisymmetric media with hp -adaptive finite elements

Christian Michler*, Leszek Demkowicz, and Carlos Torres-Verdín, University of Texas at Austin

SUMMARY

The numerical simulation of borehole acoustic measurements is of great relevance to improving the efficacy of acoustic logging techniques and to computationally estimating elastic formation properties. Such simulations require sound physical modeling combined with accurate and efficient numerical discretization and solution techniques. Our objective is to concomitantly model acoustic wave propagation in a fluid-filled borehole, elastic wave propagation in the probed rock formation, and the presence of an elastic tool used to excite wave propagation and to acquire the measurements. To ensure the accuracy and efficiency of our simulations, we use an adaptive finite-element formulation in the frequency domain enhanced with perfectly-matched-layer spatial-domain truncation. Numerical results confirm the performance and suitability of our methodology for the simulation of borehole acoustic measurements.

INTRODUCTION

Acoustic logging is a central component of the non-invasive, in-situ assessment of rock-formation properties in borehole geophysical applications, see e.g. (Tang and Cheng, 2004). The numerical simulation of problems arising in borehole acoustic logging is of great importance for advancing fundamental knowledge of borehole acoustics and for the improvement of acoustic logging techniques used by oil- and oil-service companies to detect and quantify hydrocarbon-bearing rocks. The capability of numerically simulating acoustic logging is a prerequisite for improving data inversion techniques (see e.g. (Alpak et al., 2004a,b)), such as the computational estimation of the spatial distribution of elastic formation properties from given borehole acoustic measurements. However, the simulation of borehole acoustic problems poses numerous challenges. First, the truncation of the unbounded physical domain to a bounded computational domain requires a special treatment of the truncated boundary to avoid non-physical reflections of outward traveling waves. For this purpose the *Perfectly Matched Layer* (PML) technique is commonly employed, see (Bérenger, 1994). Second, the accurate resolution of propagating waves is generally associated with a high computational cost. Third, the computational model needs to be sufficiently sophisticated to capture the essential physics while remaining computationally tractable.

Currently available simulation techniques for acoustic logging, such as those presented in (Chen et al., 1998; Liu et al., 1996; Mittet and Lasse, 1996), are typically based on finite-difference discretizations which are simple and easy to implement. However, finite differences cannot readily provide a measure of the discretization error, which limits the reliability of the numerical solution. To compensate for this lack of reliability, overly refined meshes often need to be used, since refinements that are locally confined are not possible with finite differences. This situation renders the simulation prohibitively expensive. Moreover, finite-difference methods cannot handle cases of large contrasts of elastic/acoustic properties, and they are typically restricted to simple geometries. Finally, finite differences usually entail non-physical reflections at the truncating boundary. In conclusion, current simulation methods of borehole acoustic logging can in general rightly be said to suffer from inadequate numerical techniques, which hampers further technological progress.

To accurately and efficiently simulate borehole acoustic measurements, we use an adaptive finite-element method that adapts the discretization to the local resolution requirements and delivers a reliable estimate of

the discretization error. Starting with a user-specified error tolerance, the adaptivity is carried out *automatically*, i.e. no interaction with the user is necessary, see (Demkowicz, 2005, 2006; Demkowicz et al., 2007). Such self-adaptive finite-element discretization is ideally suited to meet the above-mentioned challenges in borehole acoustic simulations. In particular, automatic adaptivity in combination with the PML technique is capable of reducing non-physical reflections from spatial domain truncation to an arbitrary level of accuracy, see (Michler et al., 2007).

Our simulations consider an axisymmetric problem with all computations carried out in the frequency domain. Numerical results confirm the suitability and reliability of our method when applied in the simulation of geometrically complex formation properties.

AUTOMATIC HP -ADAPTIVE DISCRETIZATION

To obtain an accurate solution often requires a *locally* refined discretization. Such local refinements, however, are often not supported by conventional discretization methods, such as finite differences for instance, and global refinements are generally uneconomical and expensive. To overcome this problem while retaining computational efficiency, we utilize a unique hp -adaptive finite-element software that has been developed at the University of Texas at Austin over the past 15 years; for details see (Demkowicz, 2005, 2006; Demkowicz et al., 2007). Our method is capable of adapting the discretization in terms of mesh size, h , and polynomial approximation order, p , according to the local resolution requirements of the solution. In regions where the solution varies smoothly, p -refinement is more effective than h -refinement to increase the accuracy of the approximation. Conversely, if the solution is non-smooth, h -refinement is more effective than p -refinement. To decide where and how to refine (in h or p), we construct an approximation to the discretization-error function as follows: Given an initial grid (the “*coarse grid*”), we construct a corresponding *fine grid* that we obtain by refining the coarse grid uniformly in h and p . The solution on the fine grid serves as reference solution to estimate the discretization error in the coarse-grid solution and to construct the next adaptively-refined coarse grid, and so forth. Note that, upon convergence, it is the fine-grid solution rather than the coarse-grid solution that is delivered as final solution. This *two-grid paradigm* forms a central component of our mesh-adaptation strategy. In particular, it renders the adaptivity automatic, i.e. no interaction with the user is required.

Automatic adaptivity releases the user from the burden of designing a mesh that warrants a sufficiently accurate solution. Our algorithm automatically detects changes in the solution behavior induced by material discontinuities, sources and sensors, and adapts the discretization to the local resolution requirements. Automatic adaptivity is particularly useful for enhancing the performance of the PML that is commonly used for the truncation of the computational domain, see (Bérenger, 1994). To avoid non-physical reflections, an accurate solution within the PML is indispensable. This is commonly sought after by adjusting the PML damping profile to the specific problem and discretization, typically resulting in non-trivial parameter tuning. Conversely, our automatic adaptivity adapts the discretization to an arbitrary damping profile to any user-specified error tolerance. This practically eliminates reflections from the truncation of the computational domain without parameter tuning and, hence, renders the application of the PML straightforward, see (Michler et al., 2007).

Simulation of borehole acoustic measurements

PROBLEM STATEMENT

To specify the problem under consideration, let us first state the mathematical models that we selected to describe wave propagation in borehole fluid, rock formation and logging tool.

We treat the problem in the frequency domain, assuming time-harmonic variations of the form $e^{i\omega t}$, and subsequently transform the solution back into the time domain. Solving the problem in the frequency domain offers a number of advantages over direct solution in the time domain. In particular, it obviates the stability restriction on the time-step size that is incurred by explicit time-integration methods. Moreover, it allows for the explicit consideration of frequency-dependent material properties such as those due to drilling-induced stress around the borehole. Finally, it enables us to reuse the converged mesh at a given frequency as the initial mesh for the computation at subsequent frequencies, which expedites the adaptivity and provides significant computational savings. We anticipate that a sufficiently accurate representation of the time-domain signal can be obtained by sampling between 80 and 200 representative frequencies.

We model acoustic wave propagation in a fluid-filled cylindrical borehole with the Helmholtz equation

$$-k^2 p - \Delta p = 0, \quad (1)$$

where p denotes the acoustic pressure and $k = \omega/\alpha_f$ is the wavenumber with $\omega = 2\pi f$ denoting the angular frequency and α_f the speed of sound in the fluid. We model elastic wave propagation in the rock formation surrounding the borehole and in the logging tool by the linear-elasticity equations

$$-\omega^2 \rho_s \mathbf{u} - \nabla \cdot \mathbf{S} = \mathbf{0} \quad (2)$$

$$\mathbf{S} = \lambda \mathbf{I}(\nabla \cdot \mathbf{u}) + \mu (\nabla \mathbf{u} + (\nabla \mathbf{u})^T), \quad (3)$$

where \mathbf{u} denotes the displacement vector, \mathbf{S} is the stress tensor, \mathbf{I} is the identity, ρ_s is the density of the solid, and λ and μ are the Lamé constants. The conditions at the fluid-solid interface state the compatibility of displacements and tractions at the interface which, respectively, can be expressed as

$$\nabla p \cdot \mathbf{n}_f = \rho_f \omega^2 \mathbf{u} \cdot \mathbf{n}_f \quad (4)$$

$$\mathbf{S} \cdot \mathbf{n}_s = -p \mathbf{n}_s, \quad (5)$$

where ρ_f denotes fluid density, and \mathbf{n}_f and \mathbf{n}_s are the unit outward normal vector of the fluid and the solid domain, respectively. Equation (4) relates the acoustic pressure gradient to the displacement of the solid, and Equation (5) specifies that the normal traction of the solid is in equilibrium with the fluid pressure and that the fluid does not support any shearing force. Further boundary conditions for the fluid or the solid are not required, since their respective domain is assumed to extend to infinity.

NUMERICAL RESULTS

We present numerical simulations of acoustic wave propagation in a fluid-filled borehole coupled with elastic wave propagation in a probed two-layer rock formation in the presence of an elastic logging tool.

The material data are specified in terms of the compressional-wave speed α and shear-wave speed β , which, in terms of the Lamé constants, can be expressed as

$$\alpha = \left(\frac{\lambda + 2\mu}{\rho} \right)^{1/2}, \quad \beta = \left(\frac{\mu}{\rho} \right)^{1/2}. \quad (6)$$

Tables 1 and 2 list the material, geometrical and system parameters of the problem, respectively, where R and r denote the radius of the

borehole and of the tool, respectively, and a and b denote the length of the monopole and its distance from the bottom of the mandrel, respectively. The length of the tool is 9.8 m, but for simplification we shall truncate the tool, together with the domain, at a length of 4.7 m by a PML. We consider three representative settings for the system frequency f , viz. 2, 6, and 10 kHz. The interface between the upper and lower rock formation is located at the same height as the monopole. The adopted settings are common in borehole acoustic applications.

	ρ [kg/m ³]	α [m/s]	β [m/s]
fluid	1000	1500	0
rock (upper)	2200	1700	1050
rock (lower)	2900	3000	1300
tool	7860	5100	2860

Table 1: Material properties of borehole fluid, upper (soft) and lower (hard) rock formation and logging tool.

An excitation is provided through a monopole of length a that imposes a normal pressure gradient of 13.23 GPa/m on the adjacent fluid for a frequency of 2 kHz, a pressure gradient of 357.20 GPa/m for 6 kHz and 1653.67 GPa/m for 10 kHz. All problem and load data are assumed to be axisymmetric with respect to the borehole axis, which renders the solution independent of the azimuthal coordinate and therefore enables two-dimensional computations. The dimensions of the computational domain including a 0.5 m thick PML in both radial and axial direction are $\Omega := \{(r, z) : 0m \leq r \leq 1.25m, -3.6m \leq z \leq 2.7m\}$. The PML is truncated with homogeneous Dirichlet boundary conditions. The PML damping profile is specified according to some power function that ensures a sufficiently rapid decay of the solution to machine zero over the thickness of the PML, see (Michler et al., 2007) for details. The tool occupies the subdomain $\{(r, z) : 0m \leq r \leq 0.045m, -2.5m \leq z \leq 2.7m\} =: \Omega_{\text{tool}} \subset \Omega$.

Starting from an initial mesh consisting of 3187, 7836, and 8764 degrees-of-freedom for 2, 6, and 10 kHz, respectively, an hp -mesh with 6146, 18953, and 19775 degrees-of-freedom yielding 3%, 3%, and 7% error in the H^1 -seminorm (with the fine-mesh solution used as reference solution) is obtained after 12, 18, and 10 iterations, respectively; see Figures 2 and 3.

Below, we show representative snapshots of the solution in time for frequencies of 2 kHz, 6 kHz, and 10 kHz *separately*. In our presentation, we will show the actual time-domain solution that is obtained by sampling selected frequencies and then *combining* these frequency-domain solutions upon transforming them back into the time domain. In particular, we will elaborate on frequency-sampling methods that allow us to accurately and efficiently transform the frequency-domain simulations into time-domain solutions for the detection of wave-propagation modes. A challenging aspect of this procedure pertains to the fact that the frequency-domain solutions are available on individual grids that are tailored to an optimal resolution at one particular frequency (compare the meshes shown in Figure 2 for exemplification).

Figure 1 shows snapshots in time of the radial elastic displacement in both logging tool and rock formation, and of the acoustic pressure in the borehole fluid computed on the hp -meshes given in Figure 2 for frequencies of 2, 6, and 10 kHz with a monopole source. These snapshots of the solution have been taken at time $t = T/36$ with $T = 1/f$, i.e. shortly after the logging tool has excited a pressure pulse. These figures show that waves in the borehole fluid primarily propagate in the axial (vertical) direction and, thus, the setting tool, borehole fluid,

R	r	a	b
0.1 m	0.045 m	0.02 m	2.4 m

Table 2: Geometrical parameters.

Simulation of borehole acoustic measurements

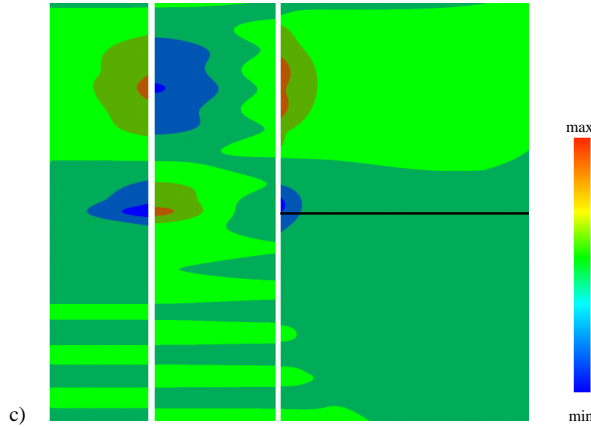
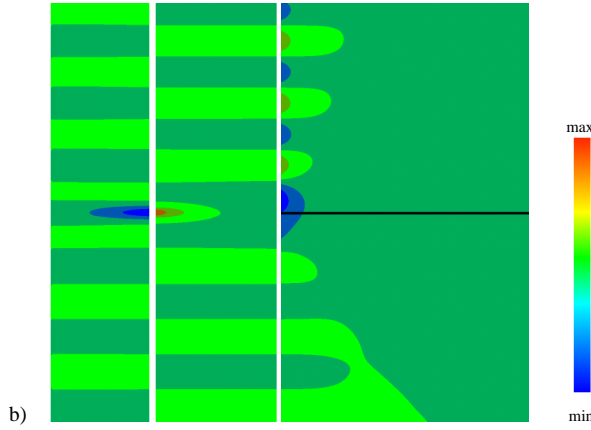
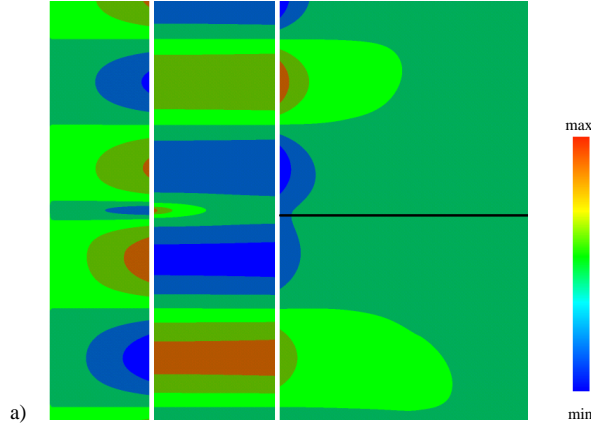


Figure 1: Snapshots of the solution at time $t = T/36$ with $T = 1/f$ for frequencies (a) $f = 2kHz$, (b) $f = 6kHz$ and (c) $f = 10kHz$ for a monopole source. From left to right: Radial displacement $u_{r,tool}$ in the logging tool, acoustic pressure p in the borehole fluid, and radial displacement $u_{r,rock}$ in the rock formation. The color bar indicates the range of the solution: (a) $u_{r,tool} [-3.26; 3.28] \times 10^{-6}m$, $p [-1.71; 1.71] \times 10^{-2}GPa$, $u_{r,rock} [-2.19; 2.11] \times 10^{-4}m$; (b) $u_{r,tool} [-27.31; 7.83] \times 10^{-6}m$, $p [-5.81; 17.88] \times 10^{-2}GPa$, $u_{r,rock} [-6.53; 4.48] \times 10^{-4}m$; (c) $u_{r,tool} [-1.78; 1.44] \times 10^{-4}m$, $p [-7.38; 10.19] \times 10^{-1}GPa$, $u_{r,rock} [-4.69; 4.56] \times 10^{-3}m$. Radial (axial) direction extends in the horizontal (vertical) direction. Moreover, for enhanced visibility of the solution, the radial coordinate in the tool and rock formation has been magnified by a factor of 10. The interface between the upper (soft) and lower (hard) rock formation has been indicated by a solid line.

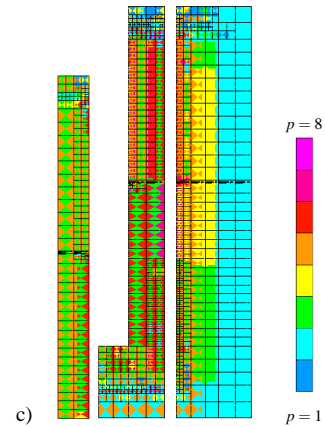
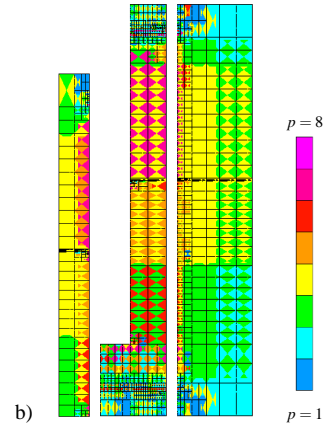
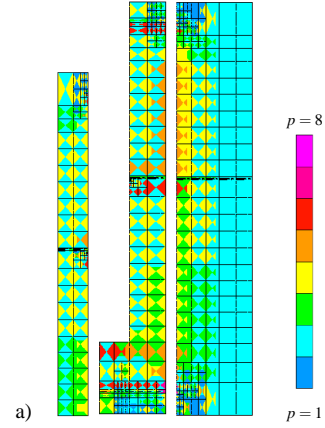


Figure 2: hp -meshes for frequencies (a) $f = 2kHz$, (b) $f = 6kHz$ and (c) $f = 10kHz$ and a monopole source. From left to right: Final hp -meshes of the tool, borehole fluid and rock formation. For enhanced visibility, the radial coordinate in the tool and rock formation has been magnified by a factor of 10. The color bar indicates the approximation order p of element edges and interiors.

Simulation of borehole acoustic measurements

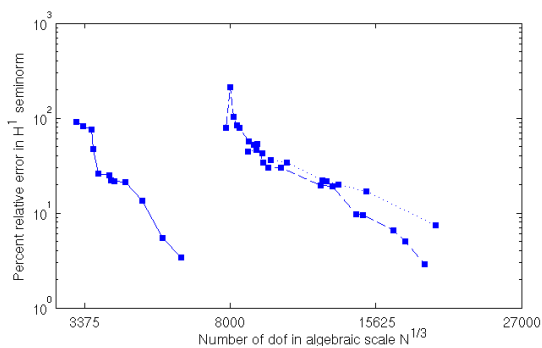


Figure 3: Convergence of the approximate solution in terms of percent relative error versus number of degrees-of-freedom for hp -adaptive refinement. Frequencies: 2 kHz (solid), 6 kHz (dashed), and 10 kHz (dotted) for a monopole source.

rock essentially acts like a waveguide in the lower and medium frequency range. This phenomenon can be attributed to the discrepancy in stiffness between the tool and rock formation on the one hand, and the borehole fluid on the other hand. Note, however, that for 10 kHz the wave propagation in the borehole fluid becomes two-dimensional in the region that is connected to the soft (upper) layer of the rock formation. Moreover, from Figure 1 the decrease in wavelength with increasing frequency is apparent, for instance the wavelength for 6 kHz is three times smaller than for 2 kHz. For a given frequency, the effect of the difference in propagation speeds in the different layers of the rock formation (see Table 1) manifests in Figure 1 in the form of different wavelengths below and above the two-layer interface. This difference in wavelengths is not only visible in the two-layer rock formation itself, but also in the acoustic borehole fluid and the elastic tool, which are both assumed homogeneous throughout their respective domain. This effect is due to the coupling between acoustic and elastic wave propagation, and it is induced by the discrepancy in wave speeds across the two-layer rock formation. Furthermore, Figure 1 indicates that, for the settings considered, the waves decay rapidly in the rock formation in the radial direction, but that they propagate along the interface between the acoustic fluid and the elastic rock formation without significant attenuation. Accordingly, Figure 2 shows that mesh refinements primarily occur along the interfaces between the acoustic fluid and the elastic rock formation and tool, respectively. Higher-order polynomial approximations have been automatically selected by the adaptive algorithm around the fluid-solid interface to effectively resolve the propagating waves (see Figure 2). In the PML region that truncates the domain in the axial direction, elements have been broken into smaller elements to efficiently resolve the sharp PML-induced solution gradients, while effectively minimizing non-physical reflections due to spatial-domain truncation. On the other hand, in the PML region that truncates the domain in the radial direction hardly any refinements are needed, since the elastic waves decay rapidly in that direction. Note that the combination of hp -adaptivity and PML practically eliminates non-physical reflections from the truncated domain boundary. Figures 2 and 3 show that the mesh for high frequencies is considerably finer and requires many more degrees-of-freedom to resolve the short-wavelength solution to the same level of accuracy than the mesh generated for lower frequencies. Finally, regarding the hp -meshes displayed in Figure 2, note that our adaptive algorithm is capable of propagating element refinements through the fluid-solid interfaces, although our formulation does allow for hanging nodes on the interface.

We are currently studying the effects of the presence of the logging tool with its particular geometrical and material properties on the wave propagation and on the acoustic signals recorded at the receivers. Nu-

merical results that assess these effects will be presented in our talk. Such investigations are important for improving acoustic logging techniques.

CONCLUSIONS

We presented the application of an hp -adaptive finite-element formulation to the simulation and study of acoustic wave propagation in a fluid-filled borehole coupled with elastic wave propagation both in a probed two-layer rock formation and in the tool used to excite the wave propagation and acquire the measurements. Numerical results confirmed the high accuracy and computational efficiency delivered by our adaptive algorithm. In particular, the combination of hp -adaptivity and PML practically eliminates non-physical reflections from the truncation of the computational domain. The simulation of borehole acoustic measurements by means of an hp -adaptive finite-element method thus appears promising.

ACKNOWLEDGEMENTS

This work was financially supported by The University of Texas at Austin's *Joint Industry Research Consortium on Formation Evaluation* sponsored by Anadarko, Aramco, Baker Atlas, BP, British Gas, Chevron, ConocoPhillips, ENI E&P, ExxonMobil, Halliburton Energy Services, Marathon Oil Corporation, Mexican Institute for Petroleum, Hydro, Occidental Petroleum Corporation, Petrobras, Schlumberger, Shell International E&P, Statoil, TOTAL, and Weatherford International Ltd. Moreover, the first author was supported by a stipend from the Netherlands Organization for Scientific Research (NWO) and by a fellowship from the Institute for Computational Engineering and Sciences of The University of Texas at Austin. This support is gratefully acknowledged.

Simulation of borehole acoustic measurements

REFERENCES

- Alpak, F., C. Torres-Verdín, and T. Habashy, 2004a, Joint inversion of transient pressure and DC resistivity measurements acquired with in-situ permanent sensors: A numerical study: *Geophysics*, **69**, 1173–1191.
- Alpak, F., C. Torres-Verdín, and K. Sepehrnooni, 2004b, Estimation of axisymmetric spatial distributions of permeability and porosity from pressure-transient data acquired with in situ permanent sensors: *Journal of Petroleum Science and Engineering*, **44**, 231–267.
- Béranger, J.-P., 1994, A perfectly matched layer for the absorption of electromagnetic waves: *Journal of Computational Physics*, **114**, 185–200.
- Chen, Y.-H., W. Chew, and Q.-H. Liu, 1998, A three-dimensional finite difference code for the modeling of sonic logging tools: *Journal of the Acoustical Society of America*, **103**, 702–712.
- Demkowicz, L., 2005, Fully automatic hp-adaptivity for Maxwell's equations: *Computer Methods in Applied Mechanics and Engineering*, **194**, 605–624.
- , 2006, Computing with hp-adaptive finite elements. I. One- and two-dimensional elliptic and Maxwell problems: CRC Press, Taylor and Francis.
- Demkowicz, L., J. Kurtz, D. Pardo, M. Paszyński, W. Rachowicz, and A. Zdunek, 2007, Computing with hp-adaptive finite elements. II. Frontiers: Three-dimensional elliptic and Maxwell problems with applications: CRC Press, Taylor and Francis.
- Liu, Q.-H., E. Schoen, F. Daube, C. Randall, and P. Lee, 1996, A three-dimensional finite difference simulation of sonic logging: *Journal of the Acoustical Society of America*, **100**, 72–79.
- Michler, C., L. Demkowicz, J. Kurtz, and D. Pardo, 2007, Improving the performance of perfectly matched layers by means of *hp*-adaptivity: *Numerical Methods for Differential Equations*. (In Press).
- Mittel, R. and R. Lasse, 1996, High-order, finite-difference modeling of multipole logging in formations with anisotropic attenuation and elasticity: *Geophysics*, **61**, 21–33.
- Tang, X.-M. and A. Cheng, 2004, Quantitative borehole acoustic methods, in Helbig, K. and S. Treitel, eds., *Handbook of geophysical exploration, Seismic exploration*, volume **24**, Elsevier.